

Preparation of Dinuclear Rhodium and Iridium Complexes with Two Bridging Hydroselenido Ligands and Their Conversion into Tri- and Tetranuclear Selenido Clusters

Hidetake Seino,[†] Yasushi Mizobe,^{*,†} and Masanobu Hidai^{*,‡}

Institute of Industrial Science, The University of Tokyo, Roppongi, Minato-ku, Tokyo 106-8558, Japan, and Department of Materials Science and Technology, Faculty of Industrial Science and Technology, Science University of Tokyo, Noda, Chiba 278-8510, Japan

Received May 12, 2000

Reactions of $[(\text{Cp}^*\text{MCl})_2(\mu\text{-Cl})_2]$ ($\text{M} = \text{Rh}$ (**4**), Ir (**5**); $\text{Cp}^* = \eta^5\text{-C}_5\text{Me}_5$) with H_2Se generated in situ from NaSeH and $\text{HCl}(\text{aq})$ in CH_2Cl_2 afforded the dirhodium and diiridium complexes containing bridging hydroselenido ligands $[(\text{Cp}^*\text{MCl})_2(\mu\text{-SeH})_2]$ ($\text{M} = \text{Rh}$ (**6**), Ir (**7**)). Complexes **6** and **7** reacted further with 0.5 equiv of **4** and **5**, respectively, to form the selenido-bridged trinuclear $\text{M}(\text{III})$ clusters $[(\text{Cp}^*\text{M})_3(\mu_3\text{-Se})_2][\text{PF}_6]_2$ ($\text{M} = \text{Rh}$ (**8**)[PF_6]₂, Ir (**9**)[PF_6]₂) after anion metathesis using $\text{K}[\text{PF}_6]$, while treatment of **6** with $[\{\text{Rh}(\text{CO})_2\}_2(\mu\text{-Cl})_2]$ or $[\text{RhCl}(\text{PPh}_3)_3]/\text{KPF}_6$ produced the trinuclear $\text{Rh}(\text{III})_2\text{Rh}(\text{I})$ clusters $[(\text{Cp}^*\text{Rh})_2\{\text{Rh}(\text{CO})_2\}(\mu_3\text{-Se})_2][\text{RhCl}_2(\text{CO})_2]$ (**10**) or $[(\text{Cp}^*\text{Rh})_2\{\text{Rh}(\text{PPh}_3)_2\}(\mu_3\text{-Se})_2][\text{PF}_6]$. On the other hand, the reactions of **6** and **7** with NEt_3 gave the tetranuclear selenido clusters with a cubane-type core $[(\text{Cp}^*\text{M})_4(\mu_3\text{-Se})_4]$ ($\text{M} = \text{Rh}$, Ir). Reactivities of **4** and **5** toward other H_2Se or SeH^- sources were also investigated, which revealed that treatment with Al_2Se_3 and H_2O in CH_2Cl_2 , followed by the anion metathesis using $\text{K}[\text{PF}_6]$, gave **8**[PF_6]₂ and **9**[PF_6]₂, respectively, as the final products, while the reactions with NaSeH in THF produced a mixture either of a cubane-type cluster $[(\text{Cp}^*\text{Rh})_4(\mu_3\text{-Se})_3(\mu_3\text{-Cl})][\text{HCl}_2]$ (**14**), **8**Cl₂, and **6** or of $[(\text{Cp}^*\text{Ir})_4(\mu_3\text{-Se})_3(\mu_2\text{-Cl})][\text{HCl}_2]$ (**15**) and **9**Cl₂. The X-ray analyses have disclosed the detailed structures for **6**, **8**[PF_6]₂, **9**[PF_6]₂, **10**, **14**, and **15**· CH_2Cl_2 .

Introduction

Transition metal–sulfur clusters have been attracting significant attention owing to their involvement in the biological and industrial catalysis.¹ However, in contrast with the rich chemistry demonstrated for the metal clusters with sulfur ligands, employment of selenium and tellurium ligands has emerged afterward.² If compared with tellurium, whose compounds often exhibit dramatic differences from the sulfur analogues, selenium does not differ very much from sulfur. Nevertheless, the larger atomic radius, slightly lower electronegativity, and more metallic nature of selenium than sulfur often result in marked changes in structures,³ electronic properties,⁴ and reactivities⁵ between metal

selenido and sulfido clusters. Among a series of selenium ligands, less attention has been paid to the hydro-selenido (HSe^-) ligand^{3b,c,6} than the monoselenido (Se^{2-}),⁷ polyselenido (Se_n^{2-} ; $n = 2\text{--}6$),⁸ and selenolato (RSe^- ; $\text{R} = \text{organic substituent}$) ligands.⁹ Hence, although a significant number of metal selenido clusters have been prepared by incorporating the metal species with certain

[†] The University of Tokyo.

[‡] Science University of Tokyo.

(1) (a) Rakowski Dubois, M. *Chem. Rev.* **1989**, *89*, 1. (b) Holm, R. H.; Ciurli, S.; Weigel, J. A. *Prog. Inorg. Chem.* **1990**, *38*, 1. (c) Krebs, B.; Henckel, G. *Angew. Chem., Int. Ed. Engl.* **1991**, *30*, 769. (d) Coucouvanis, D. *Acc. Chem. Res.* **1991**, *24*, 1. (e) Shibahara, T. *Coord. Chem. Rev.* **1993**, *123*, 73. (f) Ogino, H.; Inomata, S.; Tobita, H. *Chem. Rev.* **1998**, *98*, 2093. (g) Saito, T. *J. Chem. Soc., Dalton Trans.* **1999**, 97. (h) Fong, S.-W. A.; Hor, T. S. A. *J. Chem. Soc., Dalton Trans.* **1999**, 639. (i) Hidai, M.; Kuwata, S.; Mizobe, Y. *Acc. Chem. Res.* **2000**, *33*, 46.

(2) (a) Fenske, D.; Ohmer, J.; Hachgenei, J.; Merzweiler, K. *Angew. Chem., Int. Ed. Engl.* **1988**, *27*, 1277. (b) Wachter, A. *Angew. Chem., Int. Ed. Engl.* **1989**, *28*, 1613. (c) Ansari, M. A.; Ibers, J. A. *Coord. Chem. Rev.* **1990**, *100*, 223. (d) Roof, L. C.; Kolis, J. W. *Chem. Rev.* **1993**, *93*, 1037. (e) Dance, I.; Fisher, K. *Prog. Inorg. Chem.* **1994**, *41*, 637. (f) Hernández-Molina, R.; Sykes, A. G. *J. Chem. Soc., Dalton Trans.* **1999**, 3137.

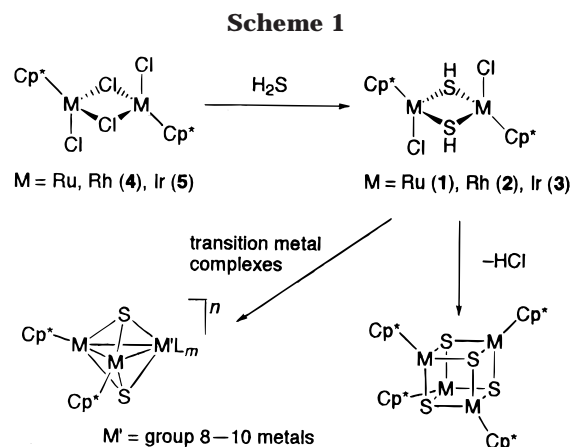
(3) (a) Brunner, H.; Meier, W.; Nuber, B.; Wachter, J.; Ziegler, M. L. *Angew. Chem., Int. Ed. Engl.* **1986**, *25*, 907. (b) Bottomley, F.; Chin, T.-T.; Egharevba, G. O.; Kane, L. M.; Pataki, D. A.; White, P. S. *Organometallics* **1988**, *7*, 1214. (c) Bottomley, F.; Day, R. W. *Organometallics* **1991**, *10*, 2560. (d) Ansari, M. A.; Chau, C.-N.; Mahler, C. H.; Ibers, J. A. *Inorg. Chem.* **1989**, *28*, 650. (e) Ellison, J. J.; Ruhlandt-Senge, K.; Hope, H. H.; Power, P. P. *Inorg. Chem.* **1995**, *34*, 49. (f) Herberhold, M.; Jin, G.-X.; Millius, W. *Chem. Ber.* **1995**, *128*, 557. (g) Inomata, S.; Hiruma, T.; Ogino, H. *Chem. Lett.* **1998**, 309. (h) Lim, B. S.; Donahue, J. P.; Holm, R. H. *Inorg. Chem.* **2000**, *39*, 263.

(4) (a) Bobrick, M. A.; Laskowski, E. J.; Johnson, R. W.; Gillum, W. O.; Berg, J. M.; Hodgson, K. O.; Holm, R. H. *Inorg. Chem.* **1978**, *17*, 1402. (b) Howard, K. E.; Rauchfuss, T. B.; Wilson, S. R. *Inorg. Chem.* **1988**, *27*, 1710. (c) Speziali, N. L.; Berger, H.; Leicht, G.; Sanjinés, R.; Chapuis, G.; Lévy, F. *Mater. Res. Bull.* **1988**, *23*, 1597. (d) Meyer, J.; Moulis, J.-M.; Gaillard, J.; Lutz, M. *Adv. Inorg. Chem.* **1992**, *38*, 73, and references therein. (e) Fischer, C.; Flechter, S.; Tributsch, H.; Reck, G.; Shultz, B. *Ber. Bunsen-Ges. Phys. Chem.* **1992**, *96*, 1652. (f) Houser, E. J.; Rauchfuss, T. B.; Wilson, S. R. *Inorg. Chem.* **1993**, *32*, 4069. (g) Oku, H.; Ueyama, N.; Nakamura, A. *Chem. Lett.* **1996**, 1131. (h) Zhou, C.; Holm, R. H. *Inorg. Chem.* **1997**, *36*, 4066. (i) Huang, J.; Mukerjee, S.; Segal, B. M.; Akashi, H.; Zhou, J.; Holm, R. H. *J. Am. Chem. Soc.* **1997**, *119*, 8662, and references therein. (j) Fedin, V. P.; Kalinina, I. V.; Samsonenko, D. G.; Mironov, Y. V.; Sokolov, M. N.; Tkachev, S. V.; Virovets, A. V.; Podberezskaya, N. V.; Elsgood, M. R. J.; Clegg, W.; Sykes, A. G. *Inorg. Chem.* **1999**, *38*, 1956.

(5) (a) Moulis, J. M.; Meyer, J. *Biochemistry* **1982**, *21*, 4762. (b) Surerus, K. K.; Kennedy, M. C.; Beinert, H.; Münck, E. *Proc. Natl. Acad. Sci. U.S.A.* **1989**, *86*, 9846.

mono- or polyselenido complexes,^{3d,4b,8c,10} those synthesized from the hydroselenido complexes are quite limited.^{6i,11}

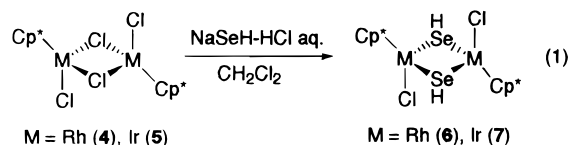
In the course of our studies to develop reliable synthetic routes leading to polymetallic clusters with designed core structures, dinuclear complexes with bridging hydrosulfido ligands such as $[(\text{Cp}^*\text{MCl})_2(\mu\text{-SH})_2]$ ($\text{Cp}^* = \eta^5\text{-C}_5\text{Me}_5$; $\text{M} = \text{Ru}$ (1),¹² Rh (2), Ir (3)¹³) have proved to serve as excellent precursors to sulfido clusters of higher nuclearity (Scheme 1). Thus, these are allowed to react with various transition metal complexes to give the sulfido-bridged trinuclear clusters of the type $[(\text{Cp}^*\text{M})_2\text{M}'\text{-L}_m(\mu_3\text{-S})_2]^n$ ($\text{M} = \text{Ru}$: $\text{M}'\text{-L}_m = \text{RhCl}_2(\text{PPh}_3)(\mu\text{-H})$,¹² $\text{RuCl}(\text{PPh}_3)_2(\mu\text{-H})$;¹⁴ $\text{M} = \text{Rh}$, Ir : $\text{M}'\text{-L}_m = \text{FeCl}_2$,¹⁵ $\text{Rh}(\text{cod})$;^{13a} $\text{M} = \text{Ir}$: $\text{M}'\text{-L}_m = \text{RuCl}_2(\text{PPh}_3)$,¹⁶ $\text{PdCl}(\text{PPh}_3)$ ^{13a}). Furthermore, treatment of 1–3 with NEt_3 produces the cubane-type sulfide clusters $[(\text{Cp}^*\text{M})_4(\mu_3\text{-S})_4]$ ($\text{M} = \text{Ru}$,¹⁴ Rh , Ir)^{13b}) through dehydrochlorination followed by dimerization. Now we have extended these studies to the systematic syntheses of



transition metal–selenido clusters using hydroselenido-bridged dinuclear species as precursors. In this paper, we wish to report the preparation of new dinuclear rhodium and iridium complexes with bridging hydroselenido ligands and the conversion of these complexes into a series of tri- and tetranuclear selenido clusters.

Results and Discussion

Reactions of $[(\text{Cp}^*\text{MCl})_2(\mu\text{-Cl})_2]$ ($\text{M} = \text{Rh}$, Ir) with H_2Se To Give Dinuclear $\mu\text{-SeH}$ Complexes. As reported previously, hydrosulfido complexes 2 and 3 are readily obtained by the reactions of $[(\text{Cp}^*\text{MCl})_2(\mu\text{-Cl})_2]$ ($\text{M} = \text{Rh}$ (4), Ir (5)) with excess H_2S gas.¹³ In the following reactions, however, since the selenium congener H_2Se is more toxic and expensive, the required amount of H_2Se was generated in situ by acidifying NaSeH ,^{6i,17} which is easier to handle than gaseous H_2Se . When 4 was allowed to react in CH_2Cl_2 at 0 °C with 2 equiv of H_2Se generated from NaSeH and aqueous HCl , the hydroselenido-bridged dirhodium complex $[(\text{Cp}^*\text{RhCl})_2(\mu\text{-SeH})_2]$ (6) was produced, which was isolated as red crystals in 62% yield. Complex 5 reacted similarly with H_2Se to give the iridium analogue $[(\text{Cp}^*\text{IrCl})_2(\mu\text{-SeH})_2]$ (7) as yellow microcrystals in 13% yield (eq 1). Due to the low stability in solution, the Ir complex 7 could not be subjected to recrystallization, which presents a marked contrast with the high stability of the Rh analogue 6 and the Ir hydrosulfido complex 3 under similar conditions.



Characterization of 6 and 7. The structure of 6 was determined in detail by single-crystal X-ray diffraction. The ORTEP drawing and important bonding parameters are shown in Figure 1. In 6, two Cp^*RhCl units are connected by the two bridging SeH ligands, where the molecule has a crystallographically imposed inversion center at the midpoint of the $\text{Rh}\text{--}\text{Rh}$ vector. Consequently, two Cp^* and two chloride ligands are each oriented trans and the two Cp^* rings are mutually parallel. For the Rh_2Se_2 plane, the $\text{Rh}\text{--}\text{Se}\text{--}\text{Rh}$ angle is

(17) Klayman, D. L.; Griffin, T. S. *J. Am. Chem. Soc.* **1973**, *95*, 197.

- (6) (a) Ugo, R.; La Monica, G.; Cenini, S.; Segre, A.; Conti, F. *J. Chem. Soc. (A)* **1971**, 522. (b) Küllmer, V.; Vahrenkamp, H. *Chem. Ber.* **1977**, *110*, 228. (c) Blacklaws, I. M.; Ebsworth, E. A. V.; Rankin, D. W. H.; Robertson, H. E. *J. Chem. Soc., Dalton Trans.* **1978**, 753. (d) Mealli, C.; Midollini, S.; Sacconi, L. *Inorg. Chem.* **1978**, *17*, 632. (e) Schmidt, M.; Hoffmann, G. G. *Z. Naturforsch.* **1978**, *33b*, 1334; *Angew. Chem., Int. Ed. Engl.* **1978**, *17*, 598. (f) Hofman, W.; Werner, H. *Angew. Chem., Int. Ed. Engl.* **1981**, *20*, 1014. (g) Hausmann, H.; Höfler, M.; Kruck, T.; Zimmermann, H. W. *Chem. Ber.* **1981**, *114*, 975. (h) Cowie, A. G.; Johnson, B. F. G.; Nicholls, J. N.; Raithby, P. R.; Rosales, M. J. *J. Chem. Soc., Dalton Trans.* **1983**, 2311. (i) Fisher, R. A.; Kneuper, H.-J.; Herrmann, W. A. *J. Organomet. Chem.* **1987**, *330*, 365. (j) Fenske, D.; Fleisher, H.; Krautscheid, H.; Magull, J.; Oliver, C.; Weisgerber, S. *Z. Naturforsch.* **1991**, *46b*, 1384. (k) Di Vaira, M.; Peruzzini, M.; Stoppioni, P. *Inorg. Chem.* **1991**, *30*, 1001. (l) Amarasakera, J.; Houser, E. J.; Rauchfuss, T. B.; Stern, C. L. *Inorg. Chem.* **1992**, *31*, 1614. (m) McDonald, R.; Cowie, M. *Inorg. Chem.* **1993**, *32*, 1671. (n) Howard, W. A.; Perkin, G. J. *Am. Chem. Soc.* **1994**, *116*, 606. (o) Mandimutsira, B. S.; Chen, S.-J.; Reynolds, R. A., III; Coucouvanis, D. *Polyhedron* **1997**, *16*, 3911. (p) Harvey, P. D.; Eichhöfer, A.; Fenske, D. *J. Chem. Soc., Dalton Trans.* **1998**, 3901. (q) Brunner, H.; Kubicki, M. M.; Leblanc, J.-C.; Meier, W.; Moise, C.; Sadorge, A.; Stubenhofer, B.; Wachter, A.; Wanninger, R. *Eur. J. Inorg. Chem.* **1999**, 843.

- (7) Perkin, G. *Prog. Inorg. Chem.* **1998**, *47*, 1.
- (8) (a) Kolis, J. W. *Coord. Chem. Rev.* **1990**, *105*, 195. (b) Kanatzidis, M. G.; Huang, S.-P. *Coord. Chem. Rev.* **1994**, *130*, 509. (c) Mathur, P. *Adv. Organomet. Chem.* **1997**, *41*, 243.

- (9) (a) Gysling, H. J. In *The Chemistry of Organic Selenium and Tellurium Compounds*; Patai, S., Rappoport, Z., Eds.; Wiley: New York, 1986; Vol. 1, p 679. (b) Arnold, J. *Prog. Inorg. Chem.* **1995**, *43*, 353.

- (10) (a) Seyferth, D.; Henderson, R. S. *J. Organomet. Chem.* **1981**, *204*, 333. (b) Day, V. W.; Lesch, D. A.; Rauchfuss, T. B. *J. Am. Chem. Soc.* **1982**, *104*, 1290. (c) Werner, H.; Luxenburger, G.; Hofmann, W.; Nadvornik, M. *J. Organomet. Chem.* **1987**, *323*, 161. (d) Saito, T.; Kajitani, Y.; Yamagata, T.; Imoto, H. *Inorg. Chem.* **1990**, *29*, 2951. (e) Mathur, P.; Hossain, M. M.; Rashid, R. S. *J. Organomet. Chem.* **1993**, *460*, 83. (f) Mathur, P.; Hossain, M. M.; Rheingold, A. L. *Organometallics*, **1994**, *13*, 3909. (g) Hong, M.; Zhang, Q.; Cao, R.; Wu, D.; Chen, J.; Zhang, W.; Liu, H.; Lu, J. *Inorg. Chem.* **1997**, *36*, 6251. (h) Shieh, M.; Tsai, Y.-C.; Cherng, J.-J.; Shieh, M.-H.; Chen, H.-S.; Ueng, C.-H.; Peng, S.-M.; Lee, G.-H. *Organometallics* **1997**, *16*, 456. (i) Cauzzi, D.; Graiff, C.; Massera, C.; Mori, G.; Predieri, G.; Tiripicchio, A. *J. Chem. Soc., Dalton Trans.* **1998**, 321. (j) Mathur, P.; Ahmed, M. O.; Dash, A. K.; Walawalkar, M. G. *J. Chem. Soc., Dalton Trans.* **1999**, 1795. (k) Nagao, S.; Seino, H.; Mizobe, Y.; Hidai, M. *Chem. Commun.* **2000**, 207.

- (11) Fischer, R. A.; Herrmann, W. A. *J. Organomet. Chem.* **1987**, *330*, 377.

- (12) Hashizume, K.; Mizobe, Y.; Hidai, M. *Organometallics* **1996**, *15*, 3303.

- (13) (a) Tang, Z.; Nomura, Y.; Ishii, Y.; Mizobe, Y.; Hidai, M. *Organometallics* **1997**, *16*, 151. (b) Tang, Z.; Nomura, Y.; Ishii, Y.; Mizobe, Y.; Hidai, M. *Inorg. Chim. Acta* **1998**, *267*, 73.

- (14) Kuwata, S.; Andou, M.; Hashizume, K.; Mizobe, Y.; Hidai, M. *Organometallics* **1998**, *17*, 3429.

- (15) Tang, Z.; Nomura, Y.; Kuwata, S.; Ishii, Y.; Mizobe, Y.; Hidai, M. *Inorg. Chem.* **1998**, *37*, 4909.

- (16) Kochi, T.; Nomura, Y.; Tang, Z.; Ishii, Y.; Mizobe, Y.; Hidai, M. *J. Chem. Soc., Dalton Trans.* **1999**, 2575.

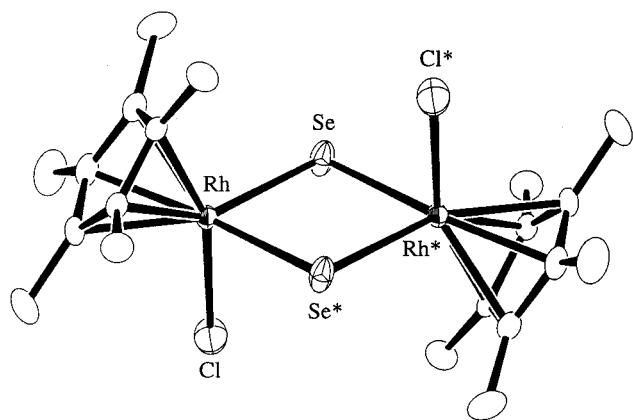


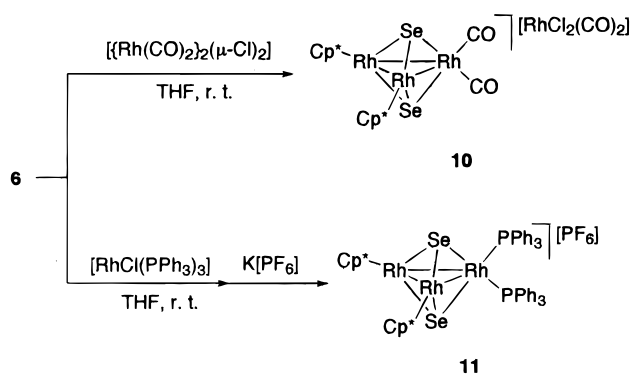
Figure 1. Molecular structure of **6**. Hydrogen atoms are omitted for clarity. Selected interatomic distances (Å) and bond angles (deg): Rh...Rh*, 3.7428(7); Rh–Se, 2.4907(7); Rh–Se*, 2.4951(7); Rh–Cl, 2.406(1); Rh–C, 2.145(4)–2.190(4); Se–Rh–Se*, 82.70(2); Se–Rh–Cl, 89.40(5); Se*–Rh–Cl, 88.94(5); Rh–Se–Rh*, 97.30(2).

slightly obtuse (97.30(2)°) and the Rh...Rh separation of 3.7428(7) Å indicates the absence of any bonding interaction between the two Rh atoms. These structural features are essentially similar to those of the SH analogue **2**¹³ and the chlorido-bridged complex **4**¹⁸ except for the longer Rh–Se bond distances at 2.4907(7) and 2.4951(7) Å than the Rh–S and Rh–Cl bond lengths in **2** (2.403(2), 2.400(2) Å) and **4** (2.465(1), 2.452(1) Å). These Rh–Se distances in **6** are comparable to those of the bridging benzeneselenolato ligands in [(CpRh)(SePh)]₂(μ-SePh)₂ (2.473(2)–2.484(2) Å) with a folded Rh₂Se₂ core.¹⁹ The hydrogen atoms bound to the selenium could not be found in the Fourier map; however, the presence of the hydroselenido protons were unambiguously demonstrated spectroscopically as described below.

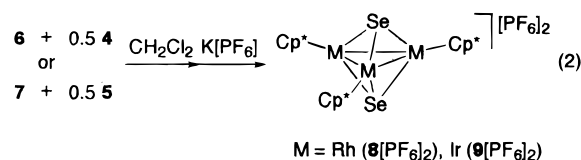
The IR spectra of **6** and **7** exhibit the characteristic ν(Se–H) bands at 2247 and 2226 cm^{−1}, respectively.²⁰ Each of their ¹H NMR spectra in C₆D₆ at 20 °C shows the presence of two isomers in solution, presumably arising from the syn and anti configurations with respect to the two SeH moieties (syn:anti = 5:3 for **6** and 3:2 for **7**). The hydroselenido protons appeared in the high-field region as the signals with the apparent ¹H–⁷⁷Se coupling: δ −2.90 (*J*_{H–Se} = 41 Hz, syn) and −2.83 (*J*_{H–Se} = 36 Hz, anti) for **6**; −2.27 (*J*_{H–Se} = 51 Hz, syn) and −2.16 (*J*_{H–Se} = 50 Hz, anti) for **7**.²¹ Similar syn–anti isomerization of the bridging SH groups is preceded for **1**,¹² **2**, and **3**.¹³

Reactions of 6 and 7 To Give the Trinuclear Selenido Clusters. The reaction of the iridium complex **7** with 0.5 equiv of **5** in CH₂Cl₂ readily proceeded at room temperature to give exclusively the product showing a Cp* resonance at δ 2.44 in CDCl₃ after 2 days. By

Scheme 2



the anion metathesis using K[PF₆], the selenido-capped triiridium cluster [(Cp*Ir)₃(μ₃-Se)₂][PF₆]₂ (**9**[PF₆]₂) was isolated in 68% yield, and its structure has been unequivocally determined by the X-ray crystallography (vide infra). Similar reaction of the Rh complex **6** with 0.5 equiv of **4** produced the Rh analogue [(Cp*Rh)₃(μ₃-Se)₂][PF₆]₂ (**8**[PF₆]₂), although the reaction was slower and the product was obtained in lower yield (30% after 6 days) (eq 2). The sulfido-capped trirhodium or tri-



iridium clusters [(Cp*M)₃(μ₃-S)₂][X]₂ (M = Rh, Ir; X = BF₄, PF₆, BPh₄) have been known for some time;²² however, their selenido analogues **8**²⁺ and **9**²⁺ are unprecedented. These reactions are assumed to proceed via liberation of HCl from **6** or **7**, forming coordinatively unsaturated dinuclear species [(Cp*M)₂(μ-Se)₂], followed by the incorporation of a Cp*M²⁺ fragment into these intermediates.

On the basis of the above reaction forming trinuclear cluster **8**²⁺ from **6**, preparation of the mixed-valent trirhodium clusters was also investigated. Thus, when **6** was allowed to react with an equimolar amount of [Rh(CO)₂]₂(μ-Cl)₂ or [RhCl(PPh₃)₃] in THF at room temperature, the trirhodium selenido clusters were isolated in moderate yields, i.e., [(Cp*Rh)₂(Rh(CO)₂)(μ₃-Se)₂][RhCl₂(CO)₂] (**10**) from the former and [(Cp*Rh)₂(Rh(PPh₃)₂)(μ₃-Se)₂][PF₆] (**11**) from the latter after treatment with K[PF₆] (Scheme 2). These clusters were spectroscopically characterized, and for **10** the structure was confirmed by the X-ray diffraction (vide infra). In the IR spectrum of **10**, four strong ν(CO) bands appeared in the region 2060–1970 cm^{−1}, for which the peaks at 2055 and 1976 cm^{−1} are characteristic of the [RhCl₂(CO)₂][−] anion,²³ while those at 2031 and 1985 cm^{−1} are assignable to the cation. These values are almost comparable to those for the other trinuclear clusters

(18) Churchill, M. R.; Julis, S. A.; Rotella, F. J. *Inorg. Chem.* **1977**, *16*, 1137.

(19) Herberhold, M.; Keller, M.; Kremnitz, W.; Daniel, T.; Milius, W.; Wrackmeyer, B.; Nöth, H. *Z. Anorg. Allg. Chem.* **1998**, *624*, 1324.

(20) The ν(Se–H) bands of the bridging hydroselenido ligands in [M(CO)₄]₂(μ-SeH)₂ (M = Mn, Re) are observed at 2223–2285 cm^{−1},^{6b} while the values reported for the terminal SeH are in the range 2250–2329 cm^{−1} except for 2526 cm^{−1} of [Et₄N][NbO(Se₂)₂(SeH)].^{6b}

(21) Previous reports show that the ¹H NMR signals of the bridging hydroselenido ligands appear in the range δ −6.35 to −3.19,^{6b,g} while those of the terminal SeH ligands are observed in the much wider range δ −6.29 to +2.68 with ¹*J*_{Se–H} = 3.3–116 Hz.

(22) (a) Venturelli, A.; Rauchfuss, T. B. *J. Am. Chem. Soc.* **1994**, *116*, 4824. (b) Nishioka, T.; Isobe, K. *Chem. Lett.* **1994**, 1661.

(23) (a) Cleare, M. J.; Griffith, W. P. *J. Chem. Soc. (A)* **1970**, 2788. (b) Cetinkaya, E.; Johnson, A. W.; Lappert, M. F.; McLaughlin, G. M.; Muir, K. W. *J. Chem. Soc., Dalton Trans.* **1974**, 1236. (c) Olmstead, M. M.; Lindsay, C. H.; Benner, L. S.; Balch, A. L. *J. Organomet. Chem.* **1979**, *179*, 289.

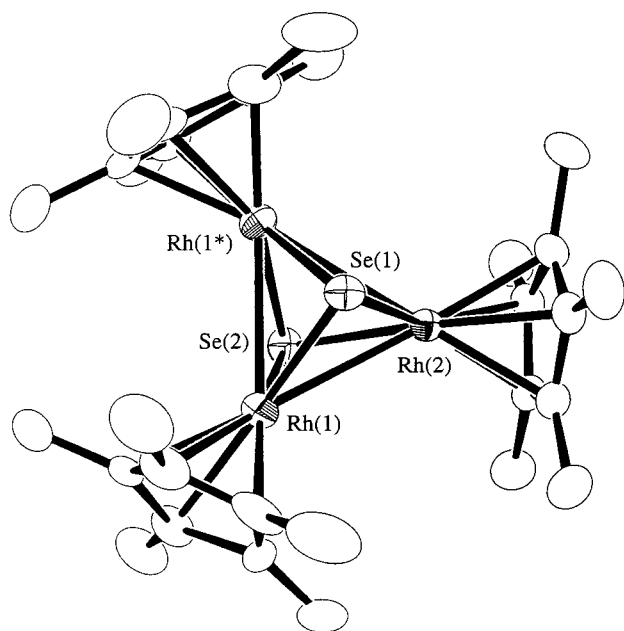


Figure 2. Structure of the cation in $8[\text{PF}_6]_2$. Hydrogen atoms are omitted for clarity.

such as $[\{\text{Rh}(\text{CO})_2\}_3(\mu_3\text{-Se})_2]^-$ (2016 and 1962 cm^{-1}),²⁴ $[\{\text{Pt}(\text{PPh}_3)_2\}_2\{\text{Rh}(\text{CO})_2\}(\mu_3\text{-S})_2][\text{PF}_6]$ (2023 and 1982 cm^{-1}),²⁵ and $[(\text{Cp}^*\text{Ir})_2\{\text{Rh}(\text{CO})_2\}(\mu_3\text{-S})_2][\text{BPh}_4]$ (2052 and 1998 cm^{-1}).²⁶ Incorporation of more diversified transition metal species into **6** and **7** is now under investigation, and the results will be reported elsewhere.

X-ray Structures of Trinuclear Clusters $8[\text{PF}_6]_2$, $9[\text{PF}_6]_2$, and **10.** Figure 2 depicts the ORTEP drawing of the cation in $8[\text{PF}_6]_2$, which is essentially identical with that of $9[\text{PF}_6]_2$, while the molecular structure of **10** is shown in Figure 3. Pertinent bonding parameters in these clusters are listed in Tables 1 and 2. Each trinuclear selenido cluster 8^{2+} , 9^{2+} , and **10** has a triangular basal plane which is capped by the selenides from both sides. Structures of 8^{2+} and 9^{2+} are closely related to their sulfido analogues $[(\text{Cp}^*\text{M})_3(\mu_3\text{-S})_2]^{2+}$ ($\text{M} = \text{Rh}, \text{Ir}$).²² Although the crystallographically imposed symmetry for 8^{2+} and 9^{2+} is only a mirror plane through the $\text{M}(2)$, $\text{Se}(1)$, and $\text{Se}(2)$ atoms, the M_3Se_2 cores have a pseudo- D_{3h} symmetry. Each Cp^*M fragment has a two-legged piano-stool geometry, if the metal–metal bonds are ignored. Distances between the metal atoms in 8^{2+} at $2.880(1)$ – $2.8879(8)\text{ Å}$ and in 9^{2+} at $2.8751(6)$ – $2.8898(8)\text{ Å}$ indicate the presence of three metal–metal bonds in each cluster, which are longer than their sulfido analogues $[(\text{Cp}^*\text{Rh})_3(\mu_3\text{-S})_2][\text{BF}_4]_2$ ($2.830(2)\text{ Å}$)^{22b} and $[(\text{Cp}^*\text{Ir})_3(\mu_3\text{-S})_2][\text{X}]_2$ ($\text{X} = \text{BF}_4$ $2.832(1)$;^{22b} $\text{X} = \text{PF}_6$ $2.8157(7)$ – $2.8201(7)\text{ Å}$)^{22a}, as well as the isoelectronic mono(μ_3 -selenido) cluster $[(\text{Cp}^*\text{Rh})_3(\mu_3\text{-Se})(\mu_3\text{-CO})]$ ($2.705(2)$ – $2.713(2)\text{ Å}$),²⁷ while the M-Se-M angles ($73.33(4)$ – $74.13(3)^\circ$) are smaller than the M-S-M angles in the above sulfido analogues (76.0 – 76.5°). As for the M-Se distances, those at $2.3969(8)$ – $2.401(1)\text{ Å}$

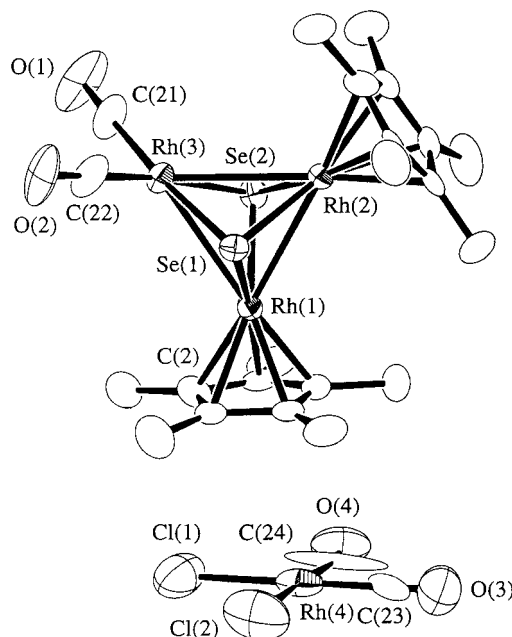


Figure 3. Molecular structure of **10**. Hydrogen atoms are omitted for clarity.

Table 1. Selected Bond Lengths (Å) and Angles (deg) in $8[\text{PF}_6]_2$ and $9[\text{PF}_6]_2$

	$8[\text{PF}_6]_2$ ($\text{M} = \text{Rh}$)	$9[\text{PF}_6]_2$ ($\text{M} = \text{Ir}$)
(a) Bond Length		
$\text{M}(1) - \text{M}(1^*)$	2.880(1)	2.8898(8)
$\text{M}(1) - \text{M}(2)$	2.8879(8)	2.8751(6)
$\text{M}(1) - \text{Se}(1)$	2.3981(8)	2.406(1)
$\text{M}(1) - \text{Se}(2)$	2.3969(8)	2.402(1)
$\text{M}(2) - \text{Se}(1)$	2.401(1)	2.409(2)
$\text{M}(2) - \text{Se}(2)$	2.395(1)	2.402(2)
$\text{M}(1) - \text{C}$	2.13(4)–2.30(3)	2.16(1)–2.22(1)
$\text{M}(2) - \text{C}$	2.171(6)–2.188(8)	2.18(1)–2.21(2)
(b) Bond Angle		
$\text{M}(1^*) - \text{M}(1) - \text{M}(2)$	60.09(1)	59.831(10)
$\text{M}(1) - \text{M}(2) - \text{M}(1^*)$	59.82(2)	60.34(2)
$\text{Se}(1) - \text{M}(1) - \text{Se}(2)$	91.98(3)	92.53(4)
$\text{Se}(1) - \text{M}(2) - \text{Se}(2)$	91.97(4)	92.45(6)
$\text{M}(1) - \text{Se}(1) - \text{M}(1^*)$	73.81(3)	73.82(5)
$\text{M}(1) - \text{Se}(1) - \text{M}(2)$	74.00(3)	73.33(4)
$\text{M}(1) - \text{Se}(2) - \text{M}(1^*)$	73.85(3)	73.96(5)
$\text{M}(1) - \text{Se}(2) - \text{M}(2)$	74.13(3)	73.51(4)

Table 2. Selected Bond Lengths (Å) and Angles (deg) in **10**

(a) Bond Length			
$\text{Rh}(1) - \text{Rh}(2)$	2.936(2)	$\text{Rh}(1) - \text{Rh}(3)$	3.007(3)
$\text{Rh}(2) - \text{Rh}(3)$	3.005(3)	$\text{Rh}(1) - \text{Se}(1)$	2.411(3)
$\text{Rh}(1) - \text{Se}(2)$	2.399(3)	$\text{Rh}(2) - \text{Se}(1)$	2.404(3)
$\text{Rh}(2) - \text{Se}(2)$	2.413(3)	$\text{Rh}(3) - \text{Se}(1)$	2.437(3)
$\text{Rh}(3) - \text{Se}(2)$	2.441(3)	$\text{Rh}(4) - \text{Cl}(1)$	2.37(1)
$\text{Rh}(4) - \text{Cl}(2)$	2.380(9)	$\text{Rh}(1) - \text{C}$	2.09(2)–2.17(2)
$\text{Rh}(2) - \text{C}$	2.16(2)–2.19(2)	$\text{Rh}(3) - \text{C}(21)$	1.89(3)
$\text{Rh}(3) - \text{C}(22)$	1.83(3)	$\text{Rh}(4) - \text{C}(23)$	1.73(3)
$\text{Rh}(4) - \text{C}(24)$	1.91(3)		
(b) Bond Angle			
$\text{Rh}(2) - \text{Rh}(1) - \text{Rh}(3)$	60.73(6)	$\text{Rh}(1) - \text{Rh}(2) - \text{Rh}(3)$	60.79(6)
$\text{Rh}(1) - \text{Rh}(3) - \text{Rh}(2)$	58.48(5)	$\text{Se}(1) - \text{Rh}(1) - \text{Se}(2)$	89.72(9)
$\text{Se}(1) - \text{Rh}(2) - \text{Se}(2)$	89.56(9)	$\text{Se}(1) - \text{Rh}(3) - \text{Se}(2)$	88.16(9)
$\text{Rh}(1) - \text{Se}(1) - \text{Rh}(2)$	75.16(8)	$\text{Rh}(1) - \text{Se}(1) - \text{Rh}(3)$	76.68(9)
$\text{Rh}(2) - \text{Se}(1) - \text{Rh}(3)$	76.74(9)	$\text{Rh}(1) - \text{Se}(2) - \text{Rh}(2)$	75.21(8)
$\text{Rh}(1) - \text{Se}(2) - \text{Rh}(3)$	76.81(9)	$\text{Rh}(2) - \text{Se}(2) - \text{Rh}(3)$	76.51(9)

in the $\text{Rh}(\text{III})$ cluster 8^{2+} and at $2.402(2)$ – $2.409(2)\text{ Å}$ in the $\text{Ir}(\text{III})$ cluster 9^{2+} are slightly shorter than those of the $\text{Rh}(\text{I})$ and $\text{Ir}(\text{I})$ clusters $[\text{NMe}_4][\{\text{M}(\text{CO})_2\}_3(\mu_3\text{-Se})_2]$ ($\text{M} = \text{Rh}$ $2.455(1)$ – $2.460(1)\text{ Å}$;²⁴ $\text{M} = \text{Ir}$ $2.477(1)$ –

(24) Galli, D.; Garlaschelli, L.; Ciani, G.; Fumagalli, A.; Martinengo, S.; Sironi, A. *J. Chem. Soc., Dalton Trans.* **1984**, 55.

(25) Gilmour, D. I.; Luke, M. A.; Mingos, M. P. *J. Chem. Soc., Dalton Trans.* **1987**, 335.

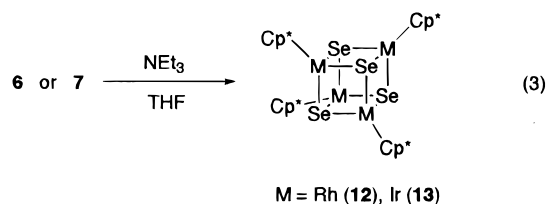
(26) Tang, Z.; Nomura, Y.; Ishii, Y.; Mizobe, Y.; Hidai, M. Unpublished result.

(27) Brunner, H.; Janietz, N.; Wachter, J.; Neumann, H.-P.; Nuber, B.; Ziegler, M. L. *J. Organomet. Chem.* **1990**, *388*, 203.

2.484(1) Å²⁸) or the cubane-type tetranuclear M(III) clusters [(Cp*M)₄(μ₃-Se)₄] (M = Rh 2.452(1)–2.471(1) Å; M = Ir 2.482(2)–2.501(2) Å).²⁹

Although no symmetry is imposed crystallographically, two Cp*Rh units and two μ₃-selenides in the cationic part of **10** are each practically equivalent and the Rh₃Se₂ core possesses C_{2v} symmetry. Neglecting the Rh–Rh interactions, the Rh(3) atom displays a square-planar geometry. Although the presence of three Rh–Rh bonds is expected from the EAN rule, the interactions between Rh(3) and the other two Rh atoms may be relatively weak, judging from the distances of 3.005(3) and 3.007(3) Å, which are intermediate between the Rh–Rh interactions in **8**²⁺ (2.880(1), 2.8879(8) Å) and those in [NMe₄][{Rh(CO)₂}₃(μ₃-Se)₂] (3.086(1)–3.159(1) Å)²⁴ with the same electron count. In addition, the Rh(1)–Rh(2) distance at 2.936(2) Å is also elongated from those in **8**²⁺. Other geometrical features around Rh(3) and the other Rh atoms are similar to those of [NMe₄][{Rh(CO)₂}₃(μ₃-Se)₂] and **8**²⁺, respectively. The anion [RhCl₂(CO)₂][−] is square-planar, which is almost parallel to the Cp* ring on Rh(1) (the dihedral angle: 3°) with the closest contact of 3.56(2) Å (Cl(1)⋯C(2)).

Reactions of 6 and 7 with NEt₃ To Give Cubane-Type Selenido Clusters. As observed for the sulfur congeners **2** and **3**, reactions of **6** and **7** with NEt₃ took place cleanly at room temperature to form the cubane-type tetranuclear selenido clusters [(Cp*M)₄(μ₃-Se)₄] (M = Rh (**12**), Ir (**13**)) in 82% and 78% yields, respectively (eq 3). These reactions are presumed to proceed via the

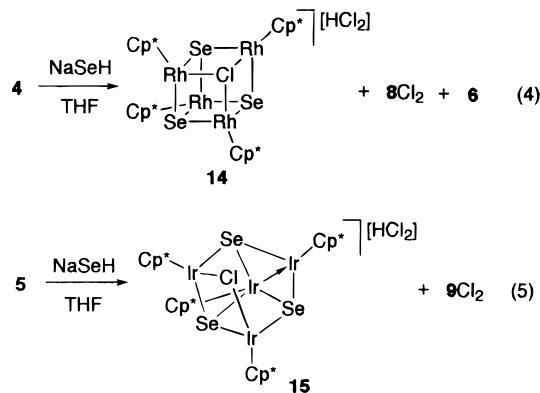


dimerization of the coordinatively unsaturated intermediates [(Cp*M)₂(μ-Se)₂] generated from **6** and **7** by treatment with NEt₃. Clusters **12** and **13** have previously been prepared by the reactions of **4** and **5** with Se(SiMe₃)₂²⁹ or the thermolysis of [{Cp*M(CO)}₂(μ-Se)₂] (M = Rh, Ir).^{3f,27}

Reactions of 4 and 5 with a Mixture of Al₂Se₃ and Water. In pursuit of the reactions forming the hydroselenido complexes, reactivities of **4** and **5** toward other H₂Se or SeH[−] sources were also investigated. When a mixture of Al₂Se₃ and H₂O was used as the H₂Se source in place of the NaSeH–HCl mixture, the reactions of **4** and **5** resulted in the formation of the trinuclear selenido clusters **8**²⁺ and **9**²⁺, which were isolated as the PF₆ salts after workup of the reaction mixture with KPF₆. When the reaction of **4** was monitored by the use of ¹H NMR spectroscopy, the resonances presumably assignable to the mono(hydroselenido) complex [(Cp*RhCl)₂(μ-SeH)(μ-Cl)]³⁰ first appeared, which gradually turned to those of **6** and then

8²⁺ over a period of 3 days. If compared with the NaSeH–HCl mixture, the Al₂Se₃–H₂O system is known to evolve H₂Se much more slowly.^{6d,h,31} Hence, in contrast with the rapid conversion of **4** into the hydroselenido complex **6** occurring in the reaction with the NaSeH–HCl mixture, the present system gradually affords **6** due to the slow generation of H₂Se. This presumably results in the successive reaction of **6** with unreacted **4** still present in the reaction mixture to give **8**²⁺ according to eq 2 described above. It is to be noted that no signals assignable to the intermediates were observed for the reaction of **5** with a Al₂Se₃–H₂O mixture, although the reaction is believed to proceed analogously. This observation may be consistent with the much higher reactivity of **7** toward **5** than that of **6** toward **4** (vide supra).

Reactions of 4 and 5 with NaSeH. Treatment of **4** and **5** with NaSeH instead of H₂Se produces new tetranuclear clusters in addition to the dinuclear and/or trinuclear complexes described above. Thus, when **4** was allowed to react with NaSeH in THF at room temperature for 2 days, the cationic cubane-type cluster [(Cp*Rh)₄(μ₃-Se)₃(μ₃-Cl)][HCl₂] (**14**) was isolated in 7% yield together with **6** and the cationic trinuclear cluster [(Cp*Rh)₃(μ₃-Se)₂]Cl₂ (**8**Cl₂) in 6% and 21% yields, respectively (eq 4). By monitoring the ¹H NMR spectral change of the reaction mixture, it turned out that the reaction of **5** with NaSeH proceeds more rapidly to give a mixture of [(Cp*Ir)₄(μ₃-Se)₃(μ-Cl)][HCl₂] (**15**) and [(Cp*Ir)₃(μ₃-Se)₂]Cl₂ (**9**Cl₂) (eq 5), although the isolated yields of these compounds were not satisfactory (5% and 11%, respectively). The formation of the hydroselenido complex was not observed in this reaction mixture. Complexes **14** and **15** might be formed from the condensation between [(Cp*M)₂(μ-Se)₂] derived from **6** and **7** by dehydrochlorination and [(Cp*MCl)₂(μ-SeH)(μ-Cl)], the Rh species of which was observed by ¹H NMR spectroscopy (vide supra).



The ¹H NMR spectrum of **14** in CDCl₃ exhibits two singlets at δ 1.54 and 1.73 in a 3:1 intensity ratio, while its FAB mass spectrum showed the parent peak of the cationic part with the expected isotopic distribution pattern. The detailed structure of **14** has finally been determined by an X-ray diffraction study as shown in Figure 4 and Table 3. Thus, **14** consists of a tetra-rhodium cluster cation with a well-separated HCl₂[−] anion. The Cl⋯Cl distance within the anion at 3.040(6) Å is comparable to those of the previously reported HCl₂[−] anions in compounds such as [CoCp₂][HCl₂]

(28) Pergola, R. D.; Garlaschelli, L.; Martinengo, S.; Demartin, F.; Manassero, M.; Sansoni, M. *J. Chem. Soc., Dalton Trans.* **1986**, 2463.

(29) Schulz, S.; Andruh, M.; Pape, T.; Heinze, T.; Roesky, H. W.; Häming, L.; Kuhn, A.; Herbst-Irmer, R. *Organometallics* **1994**, *13*, 4004.

(30) ¹H NMR (C₆D₆): δ −1.71 (t, J_{Rh–H} = 1.8 Hz, 1 H, SeH), 1.31, 1.39 (s, 15 H each, Cp*).

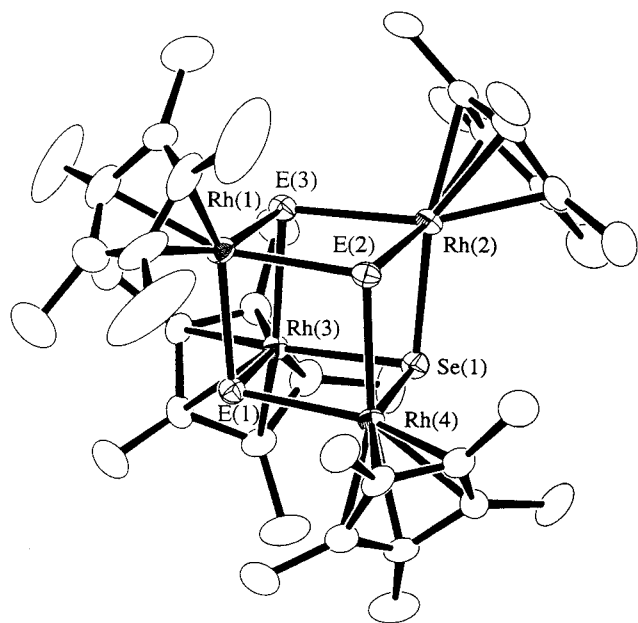


Figure 4. Structure of the cation in **14**. Hydrogen atoms are omitted for clarity. Occupancies of the disordered positions E by Se and Cl atoms are as follows: E(1), 90% Se and 10% Cl; E(2), 80% Se and 20% Cl; E(3), 30% Se and 70% Cl.

Table 3. Selected Interatomic Distances (Å) and Angles (deg) in **14^a and **15****

(a) Interatomic Distances in 14			
Rh(1)⋯Rh(2)	3.689(1)	Rh(1)⋯Rh(3)	3.6442(9)
Rh(1)⋯Rh(4)	3.710(9)	Rh(2)⋯Rh(3)	3.641(1)
Rh(2)⋯Rh(4)	3.6804(9)	Rh(3)⋯Rh(4)	3.720(1)
Rh–Se(1)	2.469(1)–2.474(1)	Rh–E	2.472(1)–2.489(2)
Rh–C	2.12(1)–2.222(9)		(av 2.478)
(b) Interatomic Angles in 14			
Se(1)–Rh–E	82.27(4)–84.96(4) (av 83.57)		
E–Rh–E	82.62(4)–85.13(4) (av 83.80)		
Rh–Se(1)–Rh	94.85(4)–97.46(4)		
Rh–E–Rh	94.44(5)–97.50(4) (av 95.90)		
(a) Interatomic Distances in 15			
Ir(1)⋯Ir(2)	3.074(2)	Ir(1)⋯Ir(3)	3.877(1)
Ir(1)⋯Ir(4)	3.842(2)	Ir(2)⋯Ir(3)	4.168(2)
Ir(2)⋯Ir(4)	4.058(2)	Ir(3)⋯Ir(4)	3.490(2)
Ir(1)–Se(1)	2.543(3)	Ir(1)–Se(2)	2.478(3)
Ir(1)–Se(3)	2.510(3)	Ir(2)–Se(1)	2.422(3)
Ir(2)–Se(2)	2.410(3)	Ir(2)⋯Cl(1)	3.11(1)
Ir(3)–Se(1)	2.526(4)	Ir(3)–Se(3)	2.483(3)
Ir(3)–Cl(1)	2.392(6)	Ir(4)–Se(2)	2.480(3)
Ir(4)–Se(3)	2.486(3)	Ir(4)–Cl(1)	2.458(7)
Ir(1)–C	2.15(3)–2.23(3)	Ir(2)–C	2.13(3)–2.29(3)
Ir(3)–C	2.15(3)–2.21(3)	Ir(4)–C	2.15(3)–2.19(3)
(b) Interatomic Angles in 15			
Se(1)–Ir(1)–Se(2)	89.61(10)	Se(1)–Ir(1)–Se(3)	78.7(1)
Se(2)–Ir(1)–Se(3)	78.70(10)	Se(1)–Ir(2)–Se(2)	94.2(1)
Se(1)–Ir(3)–Se(3)	79.6(1)	Se(1)–Ir(3)–Cl(1)	79.0(3)
Se(3)–Ir(3)–Cl(1)	86.6(2)	Se(2)–Ir(4)–Se(3)	79.13(10)
Se(2)–Ir(4)–Cl(1)	83.3(3)	Se(3)–Ir(4)–Cl(1)	85.1(2)
Ir(1)–Se(1)–Ir(2)	76.46(9)	Ir(1)–Se(1)–Ir(3)	99.8(1)
Ir(2)–Se(1)–Ir(3)	114.8(1)	Ir(1)–Se(2)–Ir(2)	77.92(9)
Ir(1)–Se(2)–Ir(4)	101.6(1)	Ir(2)–Se(2)–Ir(4)	112.2(1)
Ir(1)–Se(3)–Ir(3)	101.9(1)	Ir(1)–Se(3)–Ir(4)	100.5(1)
Ir(3)–Se(3)–Ir(4)	89.24(9)	Ir(3)–Cl(1)–Ir(4)	92.1(2)

^a For E, see the caption of Figure 4.

(3.109(3) Å)³² and [BEDT-TTF]_n[HCl₂] (*n* = 2, 3.14 Å; *n* = 1, 3.09 Å).³³ Four Cp*Rh fragments occupy the corners of the tetrahedron, whose Rh···Rh separations ranging from 3.641(1) to 3.720(1) Å are indicative of the absence

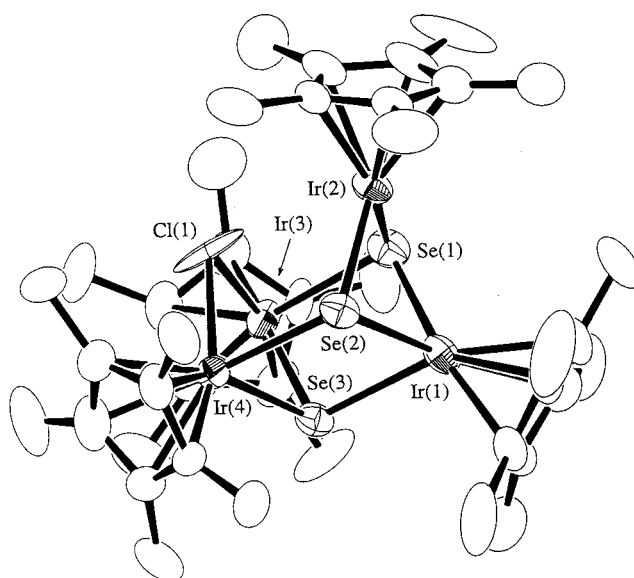


Figure 5. Structure of the cation in **15**. Hydrogen atoms are omitted for clarity.

of any Rh–Rh bonding interactions. Although some disorder is present with respect to the positions of Cl and Se atoms, it is apparent that three of the four Rh₃ faces are capped by the μ_3 -selenido ligands, with the remaining face covered by a μ_3 -chloride. The structure of this cation is quite analogous to that of **12** except for the replacement of one of the μ_3 -Se in **12** by the μ_3 -Cl in **14**. Nearly the same coordination radius of μ_3 -Se²⁻ as that of μ_3 -Cl⁻ may result in little difference between the structures of **12** and **14**.

X-ray analysis has been carried out also for **15** to confirm its structure, disclosing that the Cl···Cl distance within the anion (3.06(2) Å) is almost identical with that in **14** (3.040(6) Å). Surprisingly, despite the analogous formula of the cluster cation in **15** to that in **14**, its X-ray structure is significantly different from that of **14**, which is shown in Figure 5, and important metric parameters are listed in Table 3. Thus, the cation has a highly distorted tetrahedral core composed of four Cp*Ir fragments, of which three faces are capped with μ_3 -Se ligands. With regard to the remaining face, however, although the Cl(1) ligand is bonded to the Ir(3) and Ir(4) atoms with distances of 2.391(6) and 2.457(7) Å, respectively, the remaining Cl(1)···Ir(2) separation is quite long at 3.11(1) Å, which corresponds apparently to the nonbonding distance. Consequently, the Ir(2) atom is formally five-coordinate with a two-legged piano-stool geometry, for which the dihedral angle between the Ir(2)–Se(1)–Se(2) plane and the least-squares Cp* plane is 83.4°. The finding that the Ir(2)–Se bond distances at 2.410(3) and 2.422(3) Å are shorter than the other Ir–Se bond lengths in the range 2.478(3)–2.543(3) Å may be accounted for by the coordinatively unsaturated, electron-deficient nature of Ir(2). This is consistent with the Ir(1)···Ir(2) distance at 3.074(2) Å, which is much shorter than the other Ir···Ir separations

(31) Herberhold, M.; Jin, G.-X.; Rheingold, A. L. *Chem. Ber.* **1991**, *124*, 2245.

(32) Sens, I.; Ruhlandt-Senge, K.; Müller, U. *Acta Crystallogr.* **1992**, *C48*, 742.

(33) Ward, B. H.; Granroth, G. E.; Abboud, K. A.; Meisel, M. W.; Talham, D. R. *Chem. Mater.* **1998**, *10*, 1108. See also the references therein dealing with the salts of the HCl₂⁻ ion.

(3.490(2)–4.168(2) Å) and indicative of the presence of some bonding interaction, i.e., donation of some electron density from Ir(1) to Ir(2). The difference in the solid-state structures of **14** and **15** is in accordance with the tendency that the 16-electron complexes are more readily available for Ir than for Rh if compared under similar conditions.³⁴ The ¹H NMR spectrum in CD₂Cl₂ shows two singlets at δ 1.69 and 1.78 in an intensity ratio of 3:1, the former of which may be assigned to Ir(1) surrounded by three Se atoms and the latter to the other three Ir atoms. The equivalent nature of the latter three presumably arises from the rapid exchange of the coordination sites within the Ir(2)–Ir(3)–Ir(4) face with respect to the Cl(1) ligand.³⁵

Experimental Section

General Considerations. All manipulations were performed under nitrogen atmosphere using standard Schlenk techniques. Solvents were dried by common procedures and distilled under nitrogen before use. Complexes **4**, **5**,³⁶ [$\text{Rh}(\text{CO})_2\text{Cl}_2(\mu\text{-Cl})_2$],³⁷ [$\text{RhCl}(\text{PPh}_3)_3$],³⁸ and NaSeH^{61,17} were prepared according to literature methods. Other reagents were obtained commercially and used as received.

The ¹H (400 MHz) and ³¹P{¹H} (162 MHz) NMR spectra were recorded on a JEOL alpha-400 spectrometer, where the chemical shifts were referenced to those of the residual solvent impurities (CDCl₃ at 7.26, C₆D₆ at 7.15, and acetone-*d*₆ at 2.04 ppm) for ¹H or to external 85% H₃PO₄ (0 ppm) for ³¹P. The IR and mass spectra were recorded on JASCO FT/IR-420 and JEOL JMS600H spectrometers, respectively. Elemental analyses were done with a Perkin-Elmer 2400 series II CHN analyzer.

[(Cp*RhCl)₂(μ-SeH)₂] (6). To a suspension of **4** (675 mg, 1.09 mmol) and NaSeH (236 mg, 2.29 mmol) in CH₂Cl₂ (20 mL) was added concentrated hydrochloric acid (236 mg, 2.27 mmol) at 0 °C. The mixture was stirred at 0 °C for 1 h and then at room temperature for 30 min. The resultant mixture was dried over MgSO₄, and then hexane was added to the filtrate at –20 °C. Deposited materials were filtered off and washed with acetone and hexane to remove dark brown oil. The remaining red crystals of **6** were dried under vacuum (478 mg, 62% yield). Single crystals suitable for X-ray analyses were obtained after recrystallization from CH₂Cl₂–hexane at room temperature, although decomposition occurred slightly. ¹H NMR (C₆D₆) syn-isomer: δ –2.90 (t with ⁷⁷Se satellites, *J*_{H–Rh} = 1.6, *J*_{H–Se} = 41 Hz, 2H, SeH), 1.31, 1.47 (s, 15H each, Cp*); anti-isomer δ –2.83 (t with ⁷⁷Se satellites, *J*_{H–Rh} = 1.7, *J*_{H–Se} = 36 Hz, 2H, SeH), 1.39 (s, 30H, Cp*); syn:anti = 5:3. IR (KBr): ν(SeH), 2247 cm^{–1}. Anal. Calcd for C₂₀H₃₂Cl₂Se₂Rh₂: C, 33.97; H, 4.56. Found: C, 34.15; H, 4.17.

[(Cp*IrCl)₂(μ-SeH)₂] (7). A mixture of **5** (446 mg, 0.560 mmol), NaSeH (121 mg, 1.18 mmol), and concentrated hydrochloric acid (128 mg, 1.23 mmol) in CH₂Cl₂ (10 mL) was stirred at 0 °C for 1.5 h. The resultant solution was dried over MgSO₄, filtered, and concentrated to 2 mL at 0 °C. Deposited orange yellow crystals of **7** were filtered off, washed with acetone and hexane, and dried under vacuum (63 mg, 13% yield). Recrystallization of **7** failed owing to its severe decomposition. ¹H

NMR (C₆D₆) syn-isomer: δ –2.27 (s with ⁷⁷Se satellites, *J*_{H–Se} = 51 Hz, 2H, SeH), 1.32, 1.51 (s, 15H each, Cp*); anti-isomer δ –2.16 (s with ⁷⁷Se satellites, *J*_{H–Se} = 50 Hz, 2H, SeH), 1.41 (s, 30H, Cp*); syn:anti = 3:2. IR (KBr): ν(SeH), 2226 cm^{–1}. Anal. Calcd for C₂₀H₃₂Cl₂Se₂Ir₂: C, 27.12; H, 3.64. Found: C, 27.11; H, 3.75.

[(Cp*Rh)₃(μ₃-Se)₂][PF₆]₂ (8[PF₆]₂). **Method I.** A mixture of **4** (162 mg, 0.263 mmol), Al₂Se₃ (56.3 mg, 0.194 mmol), H₂O (22 μL, 1.2 mmol), and CH₂Cl₂ (4.5 mL) was stirred vigorously at room temperature for 3 days. The resulting dark brown solution was separated from the colorless solid by filtration, and volatiles were evaporated under reduced pressure. To the resulting black oil was added K[PF₆] (108 mg, 0.587 mmol) and CH₂Cl₂ (3 mL), and the mixture was stirred for 12 h. A dark red solid formed, which was filtered off, washed successively with water (3 × 1 mL) and THF (1 mL), and then crystallized from MeCN–ether to afford red crystals of **8[PF₆]₂** (53 mg, 26% yield). ¹H NMR (acetone-*d*₆): δ 2.09 (s, Cp*). Anal. Calcd for C₃₀H₄₅F₁₂P₂Se₂Rh₃: C, 31.00; H, 3.90. Found: C, 31.00; H, 3.92.

Method II. A CH₂Cl₂ (3 mL) solution of **6** (46 mg, 0.065 mmol) and **4** (21 mg, 0.033 mmol) was stirred at room temperature for 6 days. Addition of K[PF₆] (44 mg, 0.24 mmol) followed by a similar workup yielded **8[PF₆]₂** (23 mg, 30% yield), which was spectroscopically identical with that obtained by the above method.

[(Cp*Ir)₃(μ₃-Se)₂][PF₆]₂ (9[PF₆]₂). This complex was prepared by the methods used for the rhodium analogue **8[PF₆]₂**. The reaction for 2 days by method I or II afforded orange efflorescent crystals of **9[PF₆]₂** in 52% or 68% yield, respectively. Single crystals suitable for an X-ray diffraction study were obtained by recrystallization of these crystals from acetone–ether. ¹H NMR (acetone-*d*₆): δ 2.46 (s, Cp*). Anal. Calcd for C₃₀H₄₅F₁₂P₂Se₂Ir₃: C, 25.19; H, 3.17. Found: C, 25.17; H, 3.19.

[(Cp*Rh)₂[Rh(CO)₂](μ₃-Se)₂][RhCl₂(CO)₂] (10). Complex **6** (49 mg, 0.070 mmol) and [$\text{Rh}(\text{CO})_2\text{Cl}_2(\mu\text{-Cl})_2$] (28 mg, 0.072 mmol) in THF (7 mL) were stirred at room temperature for 12 h. The resulting dark green solution was filtered, and hexane (10 mL) was added to the concentrated (3 mL) filtrate to afford dark brown crystals of **10** (37 mg, 52% yield). ¹H NMR (CDCl₃): δ 1.84 (s, Cp*). IR (KBr): ν(CO), 2055, 2031, 1985, 1976 cm^{–1}. Anal. Calcd for C₂₄H₃₀O₄Cl₂Se₂Rh₄: C, 28.18; H, 2.96. Found: C, 28.17; H, 3.13.

[(Cp*Rh)₂[Rh(PPh₃)₂](μ₃-Se)₂][PF₆] (11). A THF (5 mL) solution of **6** (36 mg, 0.052 mmol) and [RhCl(PPh₃)₃] (49 mg, 0.052 mmol) was stirred at room temperature for 20 h. To the resulting dark reddish brown solution was added K[PF₆] (44 mg, 0.24 mmol), and the mixture was stirred continuously for a further 24 h. After filtration, the filtrate was concentrated. Addition of hexane gave black crystals of **11** (46 mg, 64% yield). ¹H NMR (CDCl₃): δ 1.72 (s, 30H, Cp*), 7.0–7.3 (m, 30H, PPh₃). ³¹P{¹H} NMR (CDCl₃): δ 34.3 (d, *J*_{PRh} = 185 Hz, PPh₃), 164.4 (sep, *J*_{P–F} = 712 Hz, PF₆). FAB MS (*m*-nitrobenzyl alcohol matrix): 1263 (cation⁺), 1000 ((cation – PPh₃)⁺) with correct isotope distribution. Anal. Calcd for C₅₆H₆₀F₆P₃Se₂Rh₃: C, 47.82; H, 4.30. Found: C, 47.53; H, 4.53.

[(Cp*Rh)₄(μ₃-Se)₄] (12). To a THF (7 mL) suspension of **6** (50 mg, 0.071 mmol) was added NEt₃ (39 μL, 0.28 mmol). After stirring the mixture for 17 h at room temperature, all volatile materials were removed under reduced pressure, and the residue was extracted with benzene. Slow diffusion of MeOH to the concentrated extract gave dark red crystals of **12** (37 mg, 82% yield), which were identical with the previously reported **12**²⁹ from the criteria of the X-ray diffraction study. ¹H NMR (C₆D₆): δ 1.77 (s, Cp*). Anal. Calcd for C₄₀H₆₀Se₄Rh₄: C, 37.88; H, 4.77. Found: C, 37.99; H, 4.77.

[(Cp*Ir)₄(μ₃-Se)₄] (13). This complex was also prepared by the method shown above in 78% yield as red crystals. Single crystals obtained by recrystallization from benzene–MeOH were not crystallographically identical with the previous

(34) (a) Garcia, J. J.; Torrens, H.; Adams, H.; Bailey, N. A.; Maitlis, P. M. *J. Chem. Soc., Chem. Commun.* **1991**, 74. (b) Garcia, J. J.; Torrens, H.; Adams, H.; Bailey, N. A.; Shacklady, A.; Maitlis, P. M. *J. Chem. Soc., Dalton Trans.* **1993**, 1529. (c) Xi, R.; Abe, M.; Suzuki, T.; Nishioka, T.; Isobe, K. *J. Organomet. Chem.* **1997**, 549, 117.

(35) Dissociation of the μ₂-Cl ligand seems to be less probable, since the treatment of **15** with K[PF₆] in CH₂Cl₂ resulted in only the metathesis of the outer sphere anion, affording the cluster with the μ₂-Cl ligand intact.

(36) White, C.; Yates, A.; Maitlis, P. M. *Inorg. Synth.* **1992**, 29, 228.

(37) Cramer, R. *Inorg. Synth.* **1974**, 15, 14.

(38) Osborn, J. A.; Wilkinson, G. *Inorg. Synth.* **1967**, 10, 67.

Table 4. Crystallographic Data for 6, 8[PF₆]₂, 9[PF₆]₂, and 10

	6	8[PF ₆] ₂	9[PF ₆] ₂	10
formula	C ₂₀ H ₃₂ Cl ₂ Se ₂ Rh ₂	C ₃₀ H ₄₅ F ₁₂ P ₂ Se ₂ Rh ₃	C ₃₀ H ₄₅ F ₁₂ P ₂ Se ₂ Ir ₃	C ₂₄ H ₃₀ O ₄ Cl ₂ Se ₂ Rh ₄
fw	707.11	1162.25	1430.19	1022.95
space group	<i>Pccn</i> (No. 56)	<i>Pnma</i> (No. 62)	<i>Pnma</i> (No. 62)	<i>Pbca</i> (No. 61)
<i>a</i> (Å)	13.512(3)	38.341(3)	14.452(5)	10.196(5)
<i>b</i> (Å)	20.435(4)	12.625(4)	12.851(2)	23.433(6)
<i>c</i> (Å)	8.660(4)	8.439(4)	21.659(3)	27.550(3)
<i>V</i> (Å ³)	2391(1)	4085(3)	4022(2)	6582(2)
<i>Z</i>	4	4	4	8
ρ _{calc} (g cm ⁻³)	1.964	1.890	2.361	2.064
<i>F</i> (000)	1376	2264	2468	3904
μ _{calc} (cm ⁻¹)	46.48	31.31	118.94	43.66
cryst size (mm ³)	0.5 × 0.3 × 0.2	0.3 × 0.3 × 0.3	0.2 × 0.2 × 0.15	0.5 × 0.25 × 0.02
scan type	ω-2θ	ω	ω-2θ	ω
2θ range (deg)	5-55	5-55	5-55	5-55
no. reflens measd	2743	4894	4828	7549
no. reflens unique	2743	4891	4825	7549
no. reflens obsd	1851	2648	3081	2480
no. var	119	380	242	326
corrections	Lorentz-polarization; abs (ψ scan, transmn factor: 0.5831-0.9989); secondary extinction (coeff: 1.3 × 10 ⁻⁷)	Lorentz-polarization; abs (ψ scan, transmn factor: 0.9103-0.9979); secondary extinction (coeff: 9.5 × 10 ⁻⁸)	Lorentz-polarization; abs (ψ scan, transmn factor: 0.6942-0.9933); secondary extinction (coeff: 1.87 × 10 ⁻⁷)	Lorentz-polarization; abs (ψ scan, transmn factor: 0.7802-0.9995); secondary extinction (coeff: 2.2 × 10 ⁻⁸)
<i>R</i> ^a	0.030	0.036	0.038	0.063
<i>R</i> _w ^b	0.032	0.033	0.040	0.065
GOF ^c	1.54	1.34	1.25	1.91
residual peaks (e ⁻ /Å ⁻³)	0.44, -0.54	0.51, -0.59	2.00, -1.45	1.10, -1.48

^a *R* = Σ||*F*_o| - |*F*_c||/Σ|*F*_o|. ^b *R*_w = [Σw(|*F*_o| - |*F*_c||)²/Σw*F*_o²]^{1/2} (*w* = [Σ(*F*_o)² + (*p*²/4)*F*_o²]⁻¹). ^c GOF = [Σw(|*F*_o| - |*F*_c||)²/(no. obsd.) - (no. var.)]^{1/2}.

Table 5. Crystallographic Data for 14 and 15·CH₂Cl₂

	14	15·CH ₂ Cl ₂
formula	C ₄₀ H ₆₁ Cl ₃ Se ₃ Rh ₄	C ₄₁ H ₆₃ Cl ₅ Se ₃ Ir ₄
fw	1296.78	1738.97
space group	<i>C2/c</i> (No. 15)	<i>P2₁/c</i> (No. 14)
<i>a</i> (Å)	17.368(1)	12.574(2)
<i>b</i> (Å)	15.053(3)	15.159(2)
<i>c</i> (Å)	35.291(2)	26.216(2)
β (deg)	93.260(6)	98.684(9)
<i>V</i> (Å ³)	9211(1)	4939(1)
<i>Z</i>	8	4
ρ _{calc} (g cm ⁻³)	1.870	2.338
<i>F</i> (000)	5072	3216
μ _{calc} (cm ⁻¹)	39.77	132.80
cryst size (mm ³)	0.7 × 0.2 × 0.1	0.4 × 0.15 × 0.15
scan type	ω	ω
2θ range (deg)	5-55	5-50
no. reflens measd	12 126	9418
no. reflens unique	10 565	8981
no. reflens obsd	5592	4363
no. var	451	479
corrections	Lorentz-polarization; abs (ψ scan, transmn factor: 0.6122-0.9996)	Lorentz-polarization; abs (ψ scan, transmn factor: 0.7576-0.9979); decay (23% decline) secondary extinction (coeff: 6.5 × 10 ⁻¹⁰)
<i>R</i> ^a	0.043	0.063
<i>R</i> _w ^b	0.043	0.074
GOF ^c	1.50	2.02
residual peaks (e ⁻ /Å ⁻³)	0.94, -0.85	2.85, -2.74

^a *R* = Σ||*F*_o| - |*F*_c||/Σ|*F*_o|. ^b *R*_w = [Σw(|*F*_o| - |*F*_c||)²/Σw*F*_o²]^{1/2} (*w* = [Σ(*F*_o)² + (*p*²/4)*F*_o²]⁻¹). ^c GOF = [Σw(|*F*_o| - |*F*_c||)²/(no. obsd.) - (no. var.)]^{1/2}.

report,²⁹ but isomorphous to those of the sulfido analogue.³⁹ ¹H NMR (C₆D₆): δ 1.72 (s, Cp*). Anal. Calcd for C₄₀H₆₀Se₄Ir₄: C, 29.55; H, 3.72. Found: C, 29.75; H, 3.73. Crystallographic data: *a* = *b* = 12.330(1), *c* = 14.874(3) Å with *Z* = 2 in space group *I*4̄ (No. 82). *R* (*R*_w) = 0.035 (0.041). GOF = 1.62 for 1239 reflections with *I* > 3σ(*I*).

[(CpRh*)₄(μ₃-Cl)(μ₃-Se)₃][HCl₂] (14).** A suspension of **4** (133 mg, 0.216 mmol) and NaSeH (44.8 mg, 0.435 mmol) in THF (8 mL) was stirred at room temperature for 2 days. The purple-red solid was filtered off, washed with THF (2 mL × 2), and then extracted with CH₂Cl₂ (2 mL × 3). On addition of hexane (6 mL) to the concentrated CH₂Cl₂ solution (3 mL), red crystals of [(Cp**Rh*)₃(μ₃-Se)₂]Cl₂ (**8**Cl₂; 29 mg, 21% yield) deposited. Further addition of hexane to the mother liquor

(39) Dobbs, D. A.; Bergman, R. G. *Inorg. Chem.* **1994**, *33*, 5329.

afforded red crystals of **6** (10 mg, 6% yield) and dark brown crystals of **14** (9 mg, 7% yield), which were separated manually. ^1H NMR (CDCl_3): δ 1.54 (s, 45H, Cp*), 1.73 (s, 15H, Cp*). FAB MS (*m*-nitrobenzyl alcohol matrix): 1225 (cation⁺) with correct isotope distribution. Anal. Calcd for $\text{C}_{40}\text{H}_{61}\text{Cl}_3\text{Se}_3\text{Rh}_4$: C, 37.05; H, 4.74. Found: C, 37.10; H, 4.53.

$[(\text{Cp}^*\text{Ir})_4(\mu\text{-Cl})(\mu_3\text{-Se})_3][\text{HCl}_2]\cdot\text{CH}_2\text{Cl}_2$ (15**· CH_2Cl_2)**. A suspension of **5** (347 mg, 0.435 mmol) and NaSeH (90 mg, 0.87 mmol) in THF (10 mL) was stirred at room temperature for 20 h. The resulting dark brown solution was filtered off, and the remaining yellow solid was extracted with THF (2.5 mL \times 4). The combined filtrate was evaporated to dryness in vacuo and redissolved in CH_2Cl_2 (4 mL). Addition of hexane (10 mL) gave orange crystals of **9**Cl₂ (38 mg, 11%). Further addition of hexane to the mother liquor afforded black crystals of **15**· CH_2Cl_2 (18 mg, 5% yield). ^1H NMR (CDCl_3): δ 1.72 (s, 45H, Cp*), 1.81 (s, 15H, Cp*). FAB MS (*m*-nitrobenzyl alcohol matrix): 1583 (cation⁺) with correct isotope distribution. Anal. Calcd for $\text{C}_{41}\text{H}_{63}\text{Cl}_5\text{Se}_3\text{Ir}_4$: C, 28.32; H, 3.65. Found: C, 28.38; H, 3.56.

X-ray Crystallography. Single crystals of **6**, **8**[PF₆]₂, **9**[PF₆]₂, **10**, **14**, and **15**· CH_2Cl_2 were sealed in glass capillaries under argon and mounted on a Rigaku AFC7R diffractometer equipped with a graphite-monochromatized Mo K α source. All diffraction studies were done at 23 °C. Orientation matrixes and unit cell parameters were determined by least-squares treatment of 25 machine-centered reflections. The intensities of three check reflections were monitored every 150 reflections during data collection, which revealed no significant decay except for **15**· CH_2Cl_2 . Details of the X-ray diffraction study are listed in Tables 4 and 5.

Structure solution and refinements were carried out by using the teXsan program package.⁴⁰ The positions of the non-hydrogen atoms were determined by Patterson methods

(PATY)⁴¹ and subsequent Fourier synthesis (DIRDIF 94).⁴² These atoms were refined by full-matrix least-squares techniques with the anisotropic thermal parameters. Chlorido and two of three selenido ligands in **14** showed signs of positional disorder, and they were refined as selenium atoms with partial atomic occupancies of 0.95, 0.90, and 0.65 to represent the approximate electron densities of 0.90 Se/0.10 Cl, 0.80 Se/0.20 Cl, and 0.30 Se/0.70 Cl, respectively. The hydrogen atoms of the hydroselenido ligand in **6** and the $[\text{HCl}_2]^-$ in **14** and **15**· CH_2Cl_2 were not found from the Fourier map and are not included. Other hydrogens were placed at the calculated positions and included in the final stages of the refinements with fixed parameters.

Acknowledgment. Financial support by the Ministry of Education, Science, Sports, and Culture of Japan (Grant Nos. 09102004 and 09238103) and The Iwatani Naoji Foundation's Research Grant is appreciated.

Supporting Information Available: X-ray crystallographic files, in CIF and PDF format, for the structure determinations of **6**, **8**[PF₆]₂, **9**[PF₆]₂, **10**, **14**, and **15**· CH_2Cl_2 are available on the Internet. This material is available free of charge via the Internet at <http://pubs.acs.org>.

OM0004040

(40) *teXsan: Crystal Structure Analysis Package*; Molecular Structure Corp.: The Woodlands, TX, 1985 and 1992.

(41) PATY: Beurskens, P. T.; Admiraal, G.; Beurskens, G.; Bosman, W. P.; Garcia-Granda, S.; Gould, R. O.; Smits, J. M. M.; Smykall, C. *The DIRDIF program system*; Technical Report of the Crystallography Laboratory: University of Nijmegen, The Netherlands, 1992.

(42) DIRDIF94: Beurskens, P. T.; Admiraal, G.; Beurskens, G.; Bosman, W. P.; de Gelder, R.; Israel, R.; Smits, J. M. M. *The DIRDIF-94 program system*; Technical Report of the Crystallography Laboratory: University of Nijmegen, The Netherlands, 1994.